

Finite-temperature second-order perturbation analysis of magnetocrystalline anisotropy energy of $L1_0$ -type ordered alloys

Shogo Yamashita * and Akimasa Sakuma 

Department of Applied Physics, Tohoku University, Sendai 980-8579, Japan



(Received 9 June 2023; accepted 24 July 2023; published 8 August 2023)

We present a finite-temperature second-order perturbation method incorporating spin-orbit coupling to investigate the temperature-dependent site-resolved contributions to the magnetocrystalline anisotropy energy (MAE), specifically $K_1(T)$, in FePt, MnAl, and FeNi alloys. Our developed method successfully reproduces the results obtained using the force theorem from our previous work. By employing this method, we identify the key sites responsible for the distinctive behaviors of MAE in these alloys, shedding light on the inadequacy of the spin model in capturing the temperature dependence of MAE in itinerant magnets. Moreover, we explore the lattice expansion effect on the temperature dependence of on-site contributions to $K_1(T)$ in FeNi. Our results not only provide insights into the limitations of the spin model in explaining the temperature dependence of MAE in itinerant ferromagnets but also highlight the need for further investigations. These findings contribute to a deeper understanding of the complex nature of MAE in itinerant magnetic systems.

DOI: [10.1103/PhysRevB.108.054411](https://doi.org/10.1103/PhysRevB.108.054411)

I. INTRODUCTION

The magnetocrystalline anisotropy energy (MAE) is an important characteristic of magnetic materials because it governs the coercivity. Rare-earth permanent magnets are examples of magnets with a high coercivity and are used for many modern applications. Recently, however, the development of rare-earth-free magnets has been accelerating to avoid the use of expensive rare-earth elements. $L1_0$ -type transition-metal alloys such as FeNi are examples of rare-earth-free high-performance permanent magnets [1]. Generally, coercivity has a strong temperature dependence; thus, we need to understand the temperature dependence of the MAE for the development of high-performance transition-metal magnets at finite temperatures.

The MAE for the uniaxial crystal $E_{\text{MAE}}(T, \theta)$ is usually expressed as follows,

$$E_{\text{MAE}}(T, \theta) = K_1(T) \sin^2 \theta + K_2(T) \sin^4 \theta + \dots, \quad (1)$$

where $K_1(T)$ and $K_2(T)$ are the anisotropy constants. However, the theoretical description of the temperature dependence of the MAE remains controversial. In localized electron systems, for instance, $4f$ electron systems such as permanent magnets, theories based on the localized spin model combined with the crystal field theory have been well established [2–8]. The Callen-Callen power law [9–12] is a line of these theories that can describe the temperature dependence of $K_1(T)$ and $K_2(T)$. In contrast, the cases of transition-metal magnets, which are treated as itinerant electron systems, are debatable. At 0 K, the mechanism of the MAE in the itinerant electron systems, particularly $K_1(0)$, can be explained by the second-order perturbation formula in terms of the spin-orbit

coupling (SOC) according to the tight-binding model [13–18]. However, finite-temperature expressions for the MAE based on the band theory are not available yet. This is because the band theory is based on the mean-field theory and cannot describe the spin-transverse fluctuations directly. One of the ways to describe the spin fluctuation based on the itinerant electron theory is the functional integral method [19–24]. This method is usually combined with the coherent potential approximation (CPA). In this approach, the spin fluctuation can be expressed by random spin states with respect to its direction, which are called disordered local moment (DLM) states. First-principles calculations based on this scheme have been performed by several authors [25–29] to investigate the finite-temperature magnetic properties of magnetic materials as pioneering works. Subsequently, the temperature dependences of the MAE, transport properties, and Gilbert damping constants in the itinerant electron systems were investigated via the DLM-CPA method and the density functional theory [30–38], along with model calculations [39–41]. In particular, the temperature dependence of the MAE for $L1_0$ -type alloys has been calculated by several authors [30–32,35]. Recently, we calculated the temperature dependence of the MAE for $L1_0$ -type FePt, MnAl, and FeNi using the DLM-CPA method [35]. The calculation results for FePt and MnAl indicated that the MAE decreases with an increase in the temperature. However, the calculated MAE for FeNi exhibited a unique behavior. It did not decrease monotonically with an increase in the temperature; rather, it exhibited plateaulike behavior in the low-temperature region. This behavior is similar to that of $\text{Y}_2\text{Fe}_{14}\text{B}$ [34,42,43], for which the mechanism of the temperature dependence of the MAE has been controversial.

In the present study, to analyze these behaviors, we decompose the MAE of these alloys at finite temperatures into on-site and pair contributions using the second-order perturbation (SOP) method in terms of the SOC. In this method, we

*shogo.yamashita.q1@dc.tohoku.ac.jp

can extend the formula to describe $K_1(0)$ in the tight-binding model [13–18] to the finite-temperature expression $K_1(T)$.

II. CALCULATION DETAILS

To develop the finite-temperature SOP formula, we use the tight-binding linearized muffin-tin orbital (TB-LMTO) method [44–48] with the atomic sphere approximation combined with the DLM-CPA method. First, in the DLM-CPA method, we need to calculate a distribution function $\omega(\{\mathbf{e}\}, T)$ representing the probability with which the spin vectors are directed to $\{\mathbf{e}\}$ at temperature T . In this work, we adopt the single-site approximation; thus, $\omega(\{\mathbf{e}\}, T)$ is decoupled into the simple product of the probability at each site $\omega_i(\mathbf{e}_i, T)$ as follows:

$$\omega(\{\mathbf{e}\}, T) = \prod_i \omega_i(\mathbf{e}_i, T). \quad (2)$$

In a previous work, $\omega_i(\mathbf{e}_i, T)$ was evaluated using the analogy of the Weiss field [28,30–32]. However, in this work, we determine $\omega_i(\mathbf{e}_i, T)$ by evaluating the effective grand potential $\Omega_{\text{eff}}(\{\mathbf{e}\}, T)$ of electrons. Here, we explain the calculation of $\Omega_{\text{eff}}(\{\mathbf{e}\}, T)$ and $\omega_i(\mathbf{e}_i, T)$. First, we introduce the Green's function including the spin-transverse fluctuation at finite temperatures in the TB-LMTO method $G(z, \{\mathbf{e}\})$ [35–38] as follows,

$$G_{ij}(z; \{\mathbf{e}\}) = \lambda_i^\beta(z; \mathbf{e}_i) \delta_{ij} + \mu_i^\beta(z; \mathbf{e}_i) g_{ij}^\beta(z; \{\mathbf{e}\}) \bar{\mu}_j^\beta(z; \mathbf{e}_j), \quad (3)$$

where z and $g_{ij}^\beta(z; \{\mathbf{e}\})$ are $E + i\delta$ and an auxiliary Green's function including spin fluctuation, respectively. $\lambda_i^\beta(z; \mathbf{e}_i)$ and $\mu_i^\beta(z; \mathbf{e}_i)$ are given as follows,

$$\lambda_i^\beta(z; \mathbf{e}_i) = [\Delta_i(\mathbf{e}_i)]^{-1/2} \{1 + [\gamma_i(\mathbf{e}_i) - \beta] P_i^\gamma(z; \mathbf{e}_i)\} [\Delta_i(\mathbf{e}_i)]^{-1/2}, \quad (4)$$

$$\mu_i^\beta(z; \mathbf{e}_i) = [\Delta_i(\mathbf{e}_i)]^{-1/2} [P_i^\gamma(z; \mathbf{e}_i)]^{-1} P_i^\beta(z; \mathbf{e}_i), \quad (5)$$

$$\bar{\mu}_i^\beta(z; \mathbf{e}_i) = P_i^\beta(z; \mathbf{e}_i) [P_i^\gamma(z; \mathbf{e}_i)]^{-1} [\Delta_i(\mathbf{e}_i)]^{-1/2}, \quad (6)$$

where

$$\Delta_i^{-1/2}(\mathbf{e}_i) = U^\dagger(\mathbf{e}_i) (\Delta_i)^{-1/2} U(\mathbf{e}_i), \quad (7)$$

$$[P_i^\gamma(z; \mathbf{e}_i)]^{-1} = U^\dagger(\mathbf{e}_i) [P_i^\gamma(z)]^{-1} U(\mathbf{e}_i), \quad (8)$$

$$\gamma_i(\mathbf{e}_i) = U^\dagger(\mathbf{e}_i) (\gamma_i) U(\mathbf{e}_i), \quad (9)$$

$$P_i^\beta(z; \mathbf{e}_i) = U^\dagger(\mathbf{e}_i) P_i^\beta(z) U(\mathbf{e}_i), \quad (10)$$

$$P_i^\beta(z) = P_i^\gamma(z) \{1 - [\beta - \gamma_i] P_i^\gamma(z)\}^{-1}, \quad (11)$$

$$P_i^\gamma(z) = (\Delta_i)^{-1/2} [z - C_i] (\Delta_i)^{-1/2}. \quad (12)$$

Here, γ_i , Δ_i , and C_i are called potential parameters in the TB-LMTO method. The β values are summarized in several papers [37,46,47]. In this work, we neglect the SOC to calculate the $\Omega_{\text{eff}}(\{\mathbf{e}\}, T)$ and $\omega_i(\mathbf{e}_i, T)$. The effective grand

potential of electronic part is expressed as

$$\begin{aligned} \Omega_{\text{eff}}(\{\mathbf{e}\}, T) &\sim \frac{1}{\pi} \int d\epsilon f(\epsilon, T, \mu) \int_{-\infty}^{\epsilon} dE \text{Im Tr } G(z; \{\mathbf{e}\}) \\ &= -\frac{1}{\pi} \int d\epsilon f(\epsilon, T, \mu) \text{Im} [\text{Tr log } \lambda^\beta(\epsilon^+; \{\mathbf{e}\}) \\ &\quad + \text{Tr log } g^\beta(\epsilon^+; \{\mathbf{e}\})], \end{aligned} \quad (13)$$

where f and μ represent the Fermi-Dirac function and the chemical potential, respectively. The trace is taken over with respect to sites i , orbitals L , and spin indices σ . From here, we expand $g^\beta(\epsilon^+; \{\mathbf{e}\})$ with the auxiliary coherent Green's function $\bar{g}^\beta(z)$, which is defined as follows,

$$\bar{g}^\beta(z) = [\bar{P}(z) - S^\beta]^{-1}, \quad (14)$$

where S^β is given as

$$S^\beta = S(1 - \beta S)^{-1}. \quad (15)$$

S is a bare structure constant matrix [45]. The auxiliary Green's function $g^\beta(\epsilon^+; \{\mathbf{e}\})$ is expanded as follows,

$$g^\beta(z; \{\mathbf{e}\}) = \bar{g}^\beta(z) (1 + \Delta P(z; \{\mathbf{e}\}) \bar{g}^\beta(z))^{-1}, \quad (16)$$

where

$$\Delta P(z; \{\mathbf{e}\}) = P^\beta(z; \{\mathbf{e}\}) - \bar{P}(z), \quad (17)$$

and \bar{P} is a coherent potential function. We also need to obtain \bar{P} in a self-consistent manner (explained later). Using Eq. (16), Eq. (13) can be rewritten as follows:

$$\begin{aligned} \Omega_{\text{eff}}(\{\mathbf{e}\}, T) &= -\frac{1}{\pi} \int d\epsilon f(\epsilon, T, \mu) \text{Im} \{ \text{Tr log } \lambda^\beta(\epsilon^+; \{\mathbf{e}\}) \\ &\quad + \text{Tr log } \bar{g}^\beta(z) - \text{Tr log} [1 + \Delta P(z; \{\mathbf{e}\}) \bar{g}^\beta(z)] \}. \end{aligned} \quad (18)$$

By taking the trace with respect to site i , the grand potential can be expressed as follows [37],

$$\Omega_{\text{eff}}(\{\mathbf{e}\}, T) = \Omega_0 + \sum_i \Delta \Omega_i(\mathbf{e}_i, T), \quad (19)$$

$$\begin{aligned} \Delta \Omega_i(\mathbf{e}_i, T) &= \frac{1}{\pi} \text{Im} \int dE f(E, T, \mu) \text{Tr}_{L\sigma} \\ &\quad \times \log [1 + \Delta P_i(z; \mathbf{e}_i) \bar{g}_{ii}^\beta(z)]. \end{aligned} \quad (20)$$

Here, we used the fact that the $\{\mathbf{e}\}$ dependence of $\lambda^\beta(\epsilon^+; \{\mathbf{e}\})$ vanishes in our case. Therefore, $\omega_i(\mathbf{e}_i, T)$ can be expressed as follows,

$$\begin{aligned} \omega_i(\mathbf{e}_i, T) &= \exp[-\Delta \Omega_i(\mathbf{e}_i, T)/k_B T] \int d\mathbf{e}_i \\ &\quad \times \exp[-\Delta \Omega_i(\mathbf{e}'_i, T)/k_B T], \end{aligned} \quad (21)$$

where k_B is the Boltzmann constant. Finally, we need to determine the converged $\omega_i(\mathbf{e}_i, T)$ and $\bar{P}(z)$ self-consistently. The

CPA condition to determine $\bar{P}(z)$ is given as

$$\int d\mathbf{e}_i \omega_i(\mathbf{e}_i, T) \Delta P_i(z; \mathbf{e}_i) [1 + \Delta P_i(z; \mathbf{e}_i) \bar{g}_{ii}^\beta(z)]^{-1} = 0. \quad (22)$$

We use Eqs. (14), (17), and (20)–(22) to obtain \bar{P}_i and the converged $\omega_i(\mathbf{e}_i, T)$ in a self-consistent manner.

Once we obtain the converged $\omega_i(\mathbf{e}_i, T)$, we can calculate the SOP formula at finite temperatures as follows,

$$\begin{aligned} \delta E^{2\text{nd}}(T, \mathbf{n}) = & -\frac{1}{2\pi} \sum_{ij} \text{Im Tr}_{L\sigma} \int_{-\infty}^{\infty} dE f(E, \mu, T) \\ & \times \langle G_{ij}(z; \{\mathbf{e}\}, \mathbf{n}) H_j^{\text{soc}} G_{ji}(z; \{\mathbf{e}\}, \mathbf{n}) H_i^{\text{soc}} \rangle_{\{\omega_i(\mathbf{e}_i, T)\}}, \end{aligned} \quad (23)$$

where H^{soc} and \mathbf{n} represent the spin-orbit Hamiltonian and the magnetization direction, respectively. Similar expressions

were used in several works [41,49]. $\langle \dots \rangle$ denotes the average over $\{\mathbf{e}\}$ with a weight of $\omega_i(\mathbf{e}_i, T)$, which is given as follows:

$$\langle \dots \rangle_{\{\omega_i(\mathbf{e}_i, T)\}} = \prod_i \int d\mathbf{e}_i \omega_i(\mathbf{e}_i, T) (\dots). \quad (24)$$

The rotation of the magnetization direction is expressed with the SO(3) rotation matrices $R(\mathbf{n})$ as follows [35,50,51],

$$S_{m_1 m_2}^{l_1 l_2}(\mathbf{n}) = \sum_{m_3 m_4} R_{m_3 m_1}^{l_1 *}(\mathbf{n}) S_{m_3 m_4}^{l_1 l_2} R_{m_4 m_2}^{l_2}(\mathbf{n}), \quad (25)$$

where $*$ denotes the complex conjugate. We substitute Eq. (25) into Eq. (14) to express the rotation of the direction of magnetization.

We can decompose Eq. (23) into on-site $E_{ii}^{2\text{nd}}$ and pair $E_{ij}^{2\text{nd}}$ contributions as follows:

$$\begin{aligned} E_{ii}^{2\text{nd}}(T, \mathbf{n}) = & -\frac{1}{2\pi} \text{Im Tr}_{L\sigma} \int d\mathbf{e}_i \omega_i(\mathbf{e}_i, T) \int_{-\infty}^{\infty} dE f(E, T, \mu) \{ H_i^{\text{soc}} [\lambda_i^\beta(z; \mathbf{e}_i) + \mu_i^\beta(z; \mathbf{e}_i) \bar{g}_{ii}^\beta(z, \mathbf{n}) \xi_i(z; \mathbf{e}_i, \mathbf{n}) \bar{\mu}_i^\beta(z; \mathbf{e}_i)] \\ & \times H_i^{\text{soc}} [\lambda_i^\beta(z; \mathbf{e}_i) + \mu_i^\beta(z; \mathbf{e}_i) \bar{g}_{ii}^\beta(z, \mathbf{n}) \xi_i(z; \mathbf{e}_i, \mathbf{n}) \bar{\mu}_i^\beta(z; \mathbf{e}_i)] \}, \end{aligned} \quad (26)$$

$$E_{ij}^{2\text{nd}}(T, \mathbf{n}) = -\frac{1}{2\pi} \sum_k \text{Im Tr}_{L\sigma} \int d\mathbf{e}_i \omega_i(\mathbf{e}_i, T) \int d\mathbf{e}'_j \omega_j(\mathbf{e}'_j, T) \int_{-\infty}^{\infty} dE f(E, T, \mu) \{ \tilde{H}_i^{\text{soc}} \chi_{ik} (1 - \Gamma \chi)_k^{-1} \tilde{H}_j^{\text{soc}} \}. \quad (27)$$

Here, we introduce $\xi_i(z; \mathbf{e}_i, \mathbf{n})$, $\tilde{\xi}_i(z; \mathbf{e}_i, \mathbf{n})$, \tilde{H}_i^{soc} , Γ , and χ , which are given as follows,

$$\xi_i(z; \mathbf{e}_i, \mathbf{n}) = [1 + \Delta P_i(z; \mathbf{e}_i) \bar{g}_{ii}^\beta(z, \mathbf{n})]^{-1}, \quad (28)$$

$$\tilde{\xi}_i(z; \mathbf{e}_i, \mathbf{n}) = [1 + \bar{g}_{ii}^\beta(z, \mathbf{n}) \Delta P_i(z; \mathbf{e}_i)]^{-1}, \quad (29)$$

$$\tilde{H}_i^{\text{soc}} = \xi_i(z; \mathbf{e}_i, \mathbf{n}) \mu_i^\beta(z; \mathbf{e}_i) H_i^{\text{soc}} \bar{\mu}_i^\beta(z; \mathbf{e}_i) \tilde{\xi}_i(z; \mathbf{e}_i, \mathbf{n}), \quad (30)$$

$$\begin{aligned} \Gamma_i(z, T, \mathbf{n}) = & \int d\mathbf{e}_i \omega_i(\mathbf{e}_i, T) [\Delta P_i^\beta(z; \mathbf{e}_i) \tilde{\xi}_i(z; \mathbf{e}_i, \mathbf{n})] \\ & \times [\Delta P_i^\beta(z; \mathbf{e}_i) \tilde{\xi}_i(z; \mathbf{e}_i, \mathbf{n})], \end{aligned} \quad (31)$$

$$\chi_{ij}(z, \mathbf{n}) = \bar{g}_{ij}^\beta(z, \mathbf{n}) \bar{g}_{ji}^\beta(z, \mathbf{n}) (1 - \delta_{ij}). \quad (32)$$

For evaluating pair contributions, we expand the Green's function including the spin fluctuation with the T matrix to include the vertex correction terms. Details regarding the derivation of the vertex correction terms are provided in several papers [38,52,53].

In practical calculations, we neglect the Fermi-Dirac distribution function in Eqs. (26) and (27). This does not cause serious numerical errors. In the present study, the $K_1(T)$ part of the MAE at finite temperatures is defined as follows:

$$K_1(T) \sim \sum_{ij} [E_{ij}^{2\text{nd}}(T, \theta = \pi/2) - E_{ij}^{2\text{nd}}(T, \theta = 0)]. \quad (33)$$

Using Eqs. (26) and (27), we can investigate the site-resolved contributions in $K_1(T)$ and its temperature dependences. For calculation details, the lattice constants of each alloy were set to $a = 2.729 \text{ \AA}$, $c = 3.706 \text{ \AA}$, $a = 2.779 \text{ \AA}$, $c = 3.56 \text{ \AA}$, and $a = 2.518 \text{ \AA}$, $c = 3.561 \text{ \AA}$ for FePt, MnAl, and FeNi,

respectively, as same as our previous work [35]. The self-consistent calculations to prepare the potential functions were performed with $25 \times 25 \times 25$ k points in the full Brillouin zone by using the local spin density approximation. The DLM calculations to prepare $\omega_i(\mathbf{e}_i, T)$ were performed with $15 \times 15 \times 15$ k points. The SOP calculations were performed with $50 \times 50 \times 50$ k points.

III. RESULTS AND DISCUSSIONS

To examine the accuracy of the developed method, let us first investigate how the SOP method can reproduce the MAE obtained via the force theorem (FT) in our previous work [35]. Figure 1 shows the MAE calculated using the FT and the SOP method for FePt, MnAl, and FeNi. Small differences between the results of the two methods are observed for FePt and FeNi, whereas little difference is observed for MnAl. For MnAl, the good agreement is reasonable, considering that the SOC of this system is far weaker than those of FePt and FeNi. From this viewpoint, the origin of the larger difference for FeNi compared with FePt is not simple, because the SOC in FeNi is weaker than that in FePt. This may suggest the peculiar $K_1(T)$ behavior of FeNi, which will be discussed later. In total summary, the qualitative behaviors of the temperature dependence of the MAE in the previous work can well be reproduced by the SOP method focusing on $K_1(T)$. The difference between the FT and the SOP method may arise from the higher-order perturbation term, which contributes to $K_2(T)$.

The total on-site and pair contributions to $K_1(T)$ are also shown in Fig. 1. For FePt, on-site and pair contributions have opposite signs for the whole temperature region. The on-site contribution is suppressed by the pair contribution, which

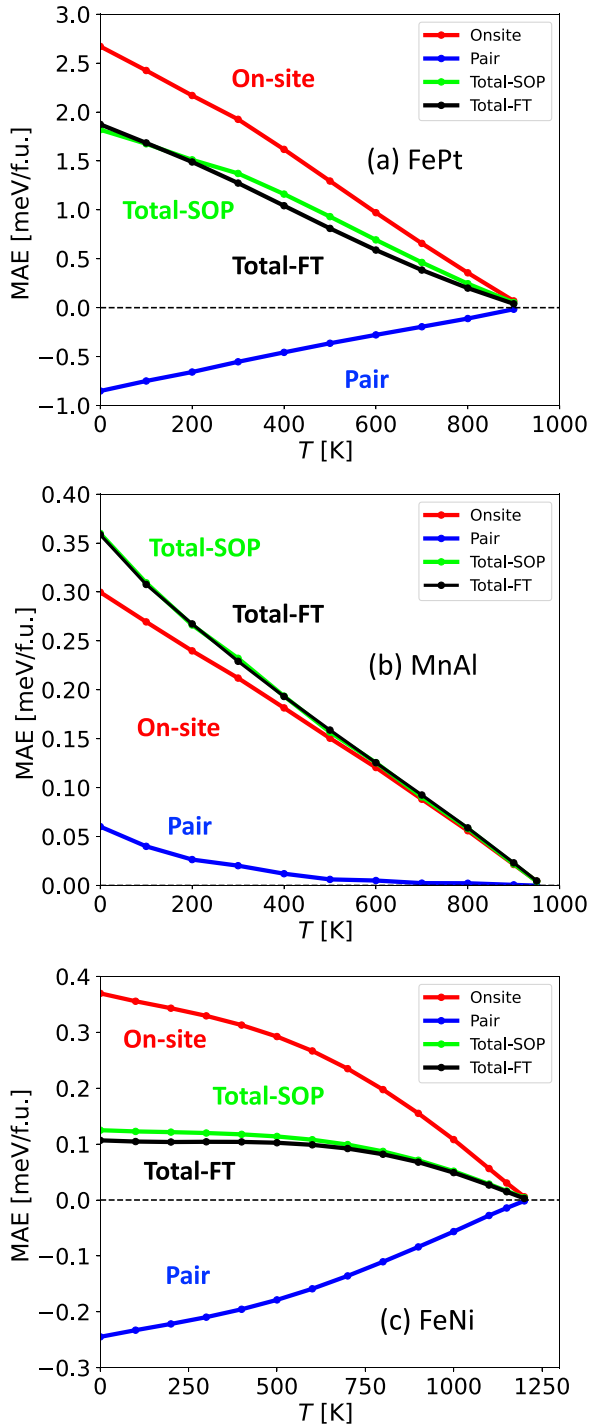


FIG. 1. Temperature dependence of the total $K_1(T)$ calculated via the developed finite-temperature SOP method including vertex correction terms for (a) FePt, (b) MnAl, and (c) FeNi, which are indicated by green lines. For comparisons, the results calculated using the FT reported by Yamashita *et al.* [35] are shown as black lines. In addition, the total on-site and total pair contributions are shown as red and blue lines, respectively.

leads to uniaxial anisotropy of $K_1(T)$. For MnAl, $K_1(T)$ is mostly dominated by the on-site contribution. The pair contribution makes a small correction to the $K_1(T)$. In this case, both contributions have a positive sign.

For FeNi, the on-site and pair contributions have similar amplitudes, whereas the signs are opposite, as in the case of FePt. In addition, the peculiar behavior that $K_1(T)$ exhibits a plateau in the low-temperature region is found to be due to the cancellation of the variations of the total on-site and total pair terms with the temperature change.

We stress here that even though the crystal structures are the same for these alloys, the alloys differ with regard to the breakdown of these SOP results into on-site and pair contributions. In particular for FePt and MnAl, despite the similar behavior of the temperature dependence of the total $K_1(T)$, the on-site and pair contributions differ significantly. Furthermore, comparing FePt and FeNi reveals that the temperature dependences of on-site and pair contributions differ significantly between these two alloys. These characteristics of the $K_1(T)$ of each alloy can be recognized via the present SOP theory at finite temperatures, which we believe is one of the advantages of this approach. It is worth mentioning that the calculated Curie temperatures are 920, 970, and 1220 K for FePt, MnAl, and FeNi, respectively. The experimental values are 750 K [54] and 653 K [55,56] for FePt and MnAl, respectively. For FeNi, the Curie temperature is estimated over 823 K [1,57]. Calculated Curie temperatures are overestimated compared with the experimental results. This might attribute to the single-site approximation, which neglects the spatial correlation of spin-transverse fluctuations. For the K_1 value of FePt, according to Okamoto *et al.* [54], 5.0 MJ/m³ was shown at room temperature (extrapolated value for ordered alloy). Our SOP result for FePt corresponds to about 6.8 MJ/m³ at 300 K. For MnAl, Nie *et al.* [58] showed 1.4 MJ/m³. Our result for MnAl is about 2.1 MJ/m³ at 0 K.

Here, to investigate the characteristics of the temperature dependence of $K_1(T)$ in the itinerant electron magnets, we compare those results with the results expected from the spin model. The Hamiltonian is given by the XXZ model [35,59–61] as follows,

$$H = - \sum_{(i,j)} 2J_{ij} \vec{S}_i \cdot \vec{S}_j - \sum_{(i,j)} D_{ij} S_i^z S_j^z - \sum_i D_i (S_i^z)^2, \quad (34)$$

where \vec{S}_i , J_{ij} , D_i , and D_{ij} are a classical spin vector, an exchange coupling constant, a single-site anisotropy coefficient, and a two-site anisotropy coefficient, respectively. As presented in our previous work [35], analysis with this model requires $D_i > 0$ and $\sum_j D_{ij} > 0$ for FePt and MnAl and $D_i < 0$ and $\sum_j D_{ij} > 0$ for FeNi to reproduce the temperature dependence of the total MAE. However, if one naively assumes that the D_i and D_{ij} terms correspond to on-site and pair contributions, respectively, at first glance, the signs of the terms in the XXZ model used in the previous work are not consistent with the results in Fig. 1, except for the case of MnAl. This mismatch originates from the fact that the temperature dependences of the MAE from the D_i and D_{ij} terms in the XXZ model behave as approximately $\propto M^3(T)$ [11,12] and $\propto M^2(T)$ [59], respectively, regardless of the signs and amplitudes of the parameters D_i and D_{ij} , whereas those of the on-site and pair terms in the SOP method do not necessarily follow such simple rules but exhibit various behaviors depending on the system. For this reason, to reproduce the peculiar

behavior of the total MAE of FeNi, the XXZ model has no other choice than to set $D_i < 0$ and $\sum_j D_{ij} > 0$; however, the on-site and pair contributions can produce such behavior with opposite signs from the XXZ model. Thus, the results in Fig. 1 imply that the spin model is too simple and is insufficient to express the temperature dependence of the MAE of itinerant magnets.

To examine each contribution in detail, we decompose the SOP results into each on-site and pair contribution. The breakdown of these contributions is shown in Fig. 2 for all the alloys. For FePt, the results are shown in Fig. 2(a). The total on-site contribution in FePt is mostly from Pt, and the Fe contribution is far smaller. In addition, it is found that the negative contribution of the total pair term in Fig. 1(a) mainly comes from the Fe-Pt pair, and it is suppressed by the positive contribution from Pt-Pt pairs. This leads to a negative total pair contribution. In this alloy, the on-site and pair contributions related to Pt significantly affect the temperature dependence of $K_1(T)$. The results for MnAl in Fig. 2(b) indicate that all the contributions are positive and that the situation regarding the total on-site term is similar to that for FePt. It is mostly dominated by the Mn on-site contribution. The second-largest contribution is the Mn-Mn positive pair contribution, and the other contributions are negligible. Thus, the on-site and pair contributions of Mn determine the temperature dependence of $K_1(T)$ in MnAl.

For FeNi, as shown in Fig. 2(c), the on-site contributions from Fe and Ni are positive and have similar amplitudes, leading to a total positive on-site contribution. We also find that the negative contribution of the total pair term mostly comes from a pair of different atoms, i.e., Fe-Ni. While the Fe-Ni contribution is suppressed by other positive pair contributions, it finally leads to negative finite total pair contributions.

From these results, although most of the pair contributions are suppressed by other pairs and the net contribution becomes small, the pair contributions play important roles over the whole temperature region, particularly for FePt and FeNi. The importance of the pair contributions was also investigated by Ke [18] with the SOP method at 0 K. In this work, we confirmed that the pair contributions to $K_1(T)$ significantly affect the temperature dependence of $K_1(T)$ at not only 0 K but also finite temperatures.

Finally, we virtually expand the lattice of FeNi to investigate the influence of electron itineracy on the on-site contribution $K_i^{\text{on}}(T)$. Here, we fit $K_i^{\text{on}}(T)$ by assuming the relation $K_i^{\text{on}}(T) \propto M_i(T)^n$ and investigate the temperature dependence of the exponent n at each site. As mentioned previously, the on-site contributions $K_i^{\text{on}}(T)$ should follow the relation $K_i^{\text{on}}(T) \propto M_i(T)^3$ if the localized spin model is suitable to explain the temperature dependence of $K_i^{\text{on}}(T)$. We briefly examine the validity of the single-site anisotropy term, which is the simplest term, for the temperature dependence of the MAE in the itinerant magnets. In Fig. 3, the temperature dependences of n of the on-site contributions for FeNi with various volumes are shown. If we expand the lattice, the n value of $K_{\text{Fe}}^{\text{on}}(T) \propto M_{\text{Fe}}(T)^n$ increases, and it reaches 3 in the low-temperature region. However, the n value of $K_{\text{Ni}}^{\text{on}}(T) \propto M_{\text{Ni}}(T)^n$ is always far from 3 and is not changed drastically. If we use a spin model with the single-site anisotropy

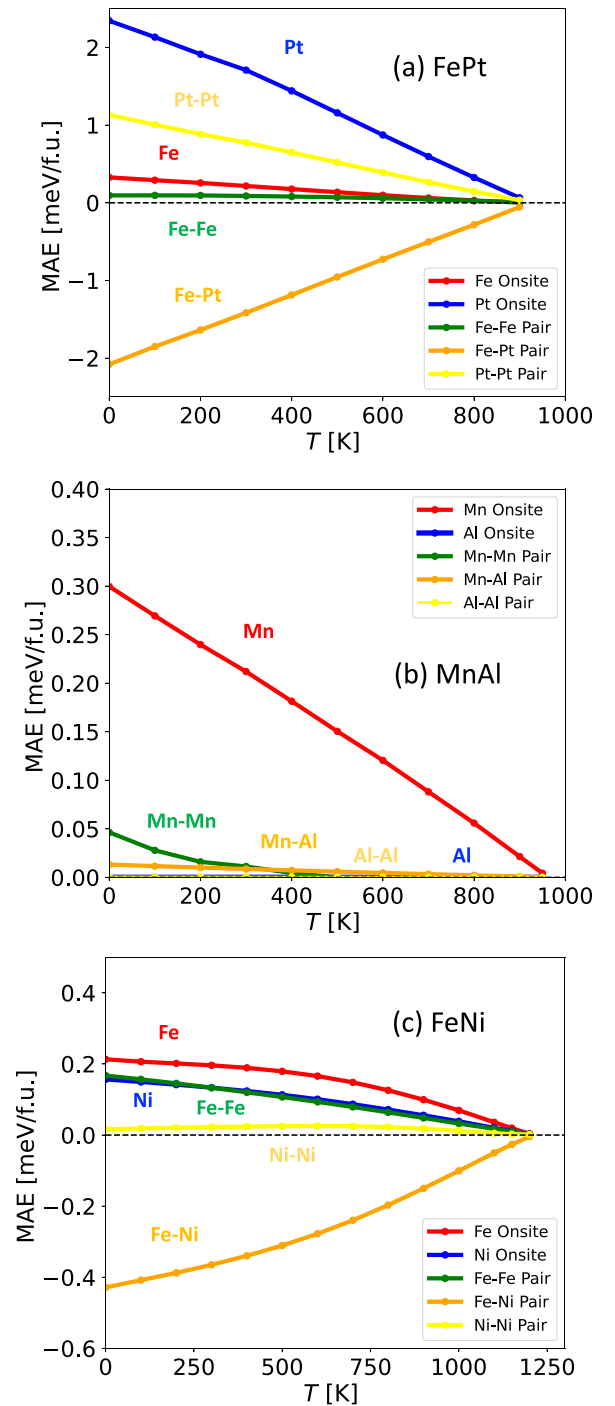


FIG. 2. Temperature dependence of the site-resolved contributions to $K_1(T)$ for (a) FePt, (b) MnAl, and (c) FeNi.

term to explain the temperature dependence of the onsite contributions, the n value must be fixed to 3 in the low-temperature region regardless of the sign and amplitude of D_i . In addition, if the lattice is expanded, the D_i and D_{ij} values are expected to change, and these temperature dependences are not changed in the localized spin model. However, our results imply that not only changing the value of D_i but also changing the temperature dependence of the on-site term itself with

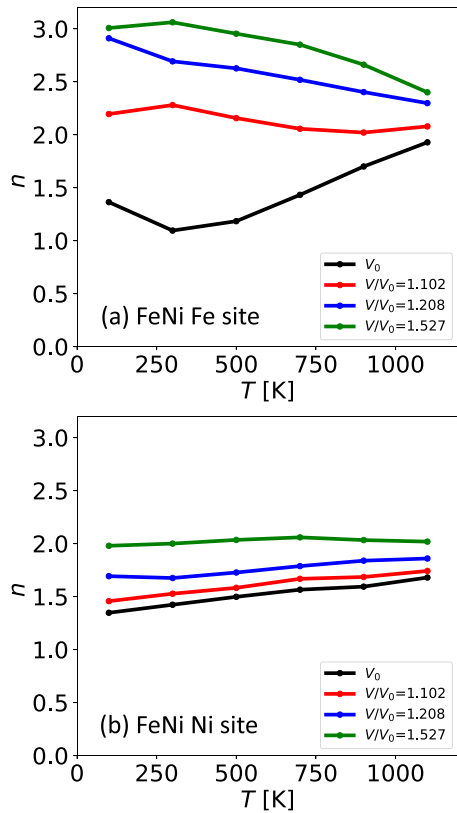


FIG. 3. Temperature dependences of the exponent n of $K_i^{\text{on}}(T)/K_i^{\text{on}}(0) = [M_i(T)/M_i(0)]^n$ for Fe and Ni sites for various volumes V of FeNi. The black line represents the results for the original volume. Other lines represent to the lattice-expanded results. V_0 is set to 22.6 \AA^3 .

expanding the lattice. Therefore, we can again conclude that if we assume Eq. (34) to explain the temperature dependence of the MAE, even the single-site anisotropy term in Eq. (34)

may not always be sufficient to describe the temperature dependence of $K_i^{\text{on}}(T)$ in the itinerant ferromagnets.

IV. SUMMARY

In summary, we developed a finite-temperature SOP method to describe the temperature dependence of $K_1(T)$ and applied it to $L1_0$ FePt, MnAl, and FeNi. We confirmed that the developed method can reproduce the results of a previous work [35]. We also investigated the on-site and pair contributions to $K_1(T)$ with the developed method. We showed that not only the on-site contributions but also the pair contributions significantly affect the temperature dependence of $K_1(T)$. In particular, the unique behavior of $K_1(T)$ for FeNi is attributed to the competition of on-site and pair-site contributions. In addition, for some results, it is found that the signs of on-site and pair contributions do not agree with the conditions used in the previous work [35]. Finally, we investigated the effect of electron itineracy for the temperature dependence of the $K_i^{\text{on}}(T)$ of FeNi while expanding the lattice parameters. We found that the exponent n of the on-site contributions of both atoms depends on the volume and is not fixed to 3, which is expected from a spin model. From the above, our results imply that the XXZ model, even the single-site anisotropy term in this model, is insufficient for the itinerant ferromagnets.

ACKNOWLEDGMENTS

S.Y. acknowledges Dr. Ryoya Hiramatsu, Dr. Yusuke Masaki, and Prof. Dr. Hiroaki Matsueda of Tohoku University for fruitful discussions and support from GP-Spin at Tohoku University, Japan. S.Y. also appreciates Dr. Juba Bouaziz and Professor Dr. Stefan Blügel of Forschungszentrum Jülich for constructive comments on this work. This work was supported by JSPS KAKENHI Grant No. JP19H05612 in Japan.

- [1] S. Goto, H. Kura, E. Watanabe, Y. Hayashi, H. Yanagihara, Y. Shimada, M. Mizuguchi, K. Takanashi, and E. Kita, *Sci. Rep.* **7**, 13216 (2017).
- [2] J. F. Herbst, *Rev. Mod. Phys.* **63**, 819 (1991).
- [3] M. Yamada, H. Kato, H. Yamamoto, and Y. Nakagawa, *Phys. Rev. B* **38**, 620 (1988).
- [4] R. Sasaki, D. Miura, and A. Sakuma, *Appl. Phys. Express* **8**, 043004 (2015).
- [5] T. Yoshioka and H. Tsuchiura, *Appl. Phys. Lett.* **112**, 162405 (2018).
- [6] T. Yoshioka, H. Tsuchiura, and P. Novák, *Phys. Rev. B* **102**, 184410 (2020).
- [7] S. Yamashita, D. Suzuki, T. Yoshioka, H. Tsuchiura, and P. Novák, *Phys. Rev. B* **102**, 214439 (2020).
- [8] T. Yoshioka, H. Tsuchiura, and P. Novák, *Phys. Rev. B* **105**, 014402 (2022).
- [9] N. Akulov, *Z. Phys.* **100**, 197 (1936).
- [10] C. Zener, *Phys. Rev.* **96**, 1335 (1954).
- [11] E. R. Callen and H. B. Callen, *Phys. Rev.* **129**, 578 (1963).
- [12] E. R. Callen and H. B. Callen, *J. Phys. Chem. Solids* **27**, 1271 (1966).
- [13] P. Bruno, *Phys. Rev. B* **39**, 865 (1989).
- [14] G. van der Laan, *J. Phys.: Condens. Matter* **10**, 3239 (1998).
- [15] Y. Kota and A. Sakuma, *J. Phys. Soc. Jpn.* **83**, 034715 (2014).
- [16] I. V. Solovyev, P. H. Dederichs, and I. Mertig, *Phys. Rev. B* **52**, 13419 (1995).
- [17] L. Ke and M. van Schilfgaarde, *Phys. Rev. B* **92**, 014423 (2015).
- [18] L. Ke, *Phys. Rev. B* **99**, 054418 (2019).
- [19] M. Cyrot, *Phys. Rev. Lett.* **25**, 871 (1970).
- [20] J. Hubbard, *Phys. Rev. B* **19**, 2626 (1979).
- [21] J. Hubbard, *Phys. Rev. B* **20**, 4584 (1979).
- [22] H. Hasegawa, *J. Phys. Soc. Jpn.* **46**, 1504 (1979).
- [23] H. Hasegawa, *J. Phys. Soc. Jpn.* **49**, 178 (1980).
- [24] H. Hasegawa, *J. Phys. Soc. Jpn.* **49**, 963 (1980).
- [25] T. Oguchi, K. Terakura, and N. Hamada, *J. Phys. F: Met. Phys.* **13**, 145 (1983).
- [26] A. J. Pindor, J. Staunton, G. M. Stocks, and H. Winter, *J. Phys. F: Met. Phys.* **13**, 979 (1983).

- [27] J. Staunton, B. L. Gyorffy, A. J. Pindor, G. M. Stocks, and H. Winter, *J. Magn. Magn. Mater.* **45**, 15 (1984).
- [28] B. L. Gyorffy, A. J. Pindor, J. Staunton, G. M. Stocks, and H. Winter, *J. Phys. F: Met. Phys.* **15**, 1337 (1985).
- [29] J. B. Staunton and B. L. Gyorffy, *Phys. Rev. Lett.* **69**, 371 (1992).
- [30] J. B. Staunton, S. Ostanin, S. S. A. Razee, B. L. Gyorffy, L. Szunyogh, B. Ginatempo, and E. Bruno, *Phys. Rev. Lett.* **93**, 257204 (2004).
- [31] J. B. Staunton, L. Szunyogh, A. Buruzs, B. L. Gyorffy, S. Ostanin, and L. Udvardi, *Phys. Rev. B* **74**, 144411 (2006).
- [32] A. Deák, E. Simon, L. Balogh, L. Szunyogh, M. dos Santos Dias, and J. B. Staunton, *Phys. Rev. B* **89**, 224401 (2014).
- [33] M. Matsumoto, R. Banerjee, and J. B. Staunton, *Phys. Rev. B* **90**, 054421 (2014).
- [34] J. Bouaziz, C. E. Patrick, and J. B. Staunton, *Phys. Rev. B* **107**, L020401 (2023).
- [35] S. Yamashita and A. Sakuma, *J. Phys. Soc. Jpn.* **91**, 093703 (2022).
- [36] R. Hiramatsu, D. Miura, and A. Sakuma, *Appl. Phys. Express* **15**, 013003 (2022).
- [37] A. Sakuma and D. Miura, *J. Phys. Soc. Jpn.* **91**, 084701 (2022).
- [38] R. Hiramatsu, D. Miura, and A. Sakuma, *J. Phys. Soc. Jpn.* **92**, 044704 (2023).
- [39] A. Sakuma, *J. Phys. Soc. Jpn.* **87**, 034705 (2018).
- [40] D. Miura and A. Sakuma, *J. Phys. Soc. Jpn.* **90**, 113601 (2021).
- [41] D. Miura and A. Sakuma, *J. Phys. Soc. Jpn.* **91**, 023706 (2022).
- [42] M. Sagawa, S. Fujimura, H. Yamamoto, Y. Matsuura, and S. Hirose, *J. Appl. Phys.* **57**, 4094 (1985).
- [43] R. Grössinger, X. Sun, R. Eibler, K. Buschow, and H. Kirchmayr, *J. Magn. Magn. Mater.* **58**, 55 (1986).
- [44] O. K. Andersen, Z. Pawłowska, and O. Jepsen, *Phys. Rev. B* **34**, 5253 (1986).
- [45] H. L. Skriver, *The LMTO Method* (Springer, Berlin, 1984).
- [46] I. Turek, V. Drchal, J. Kudrnovský, M. Šöb, and P. Weinberger, *Electronic Structure of Disordered Alloys, Surfaces and Interfaces* (Kluwer Academic, Dordrecht, 1997).
- [47] J. Kudrnovský and V. Drchal, *Phys. Rev. B* **41**, 7515 (1990).
- [48] A. Sakuma, *J. Phys. Soc. Jpn.* **69**, 3072 (2000).
- [49] N. Kobayashi, Y. Kota, and A. Sakuma, *J. Phys. Soc. Jpn.* **87**, 094714 (2018).
- [50] H. Ebert, *Phys. Rev. B* **38**, 9390 (1988).
- [51] A. Sakuma, *J. Phys. Soc. Jpn.* **63**, 1422 (1994).
- [52] W. H. Butler, *Phys. Rev. B* **31**, 3260 (1985).
- [53] K. Carva, I. Turek, J. Kudrnovský, and O. Bengone, *Phys. Rev. B* **73**, 144421 (2006).
- [54] S. Okamoto, N. Kikuchi, O. Kitakami, T. Miyazaki, Y. Shimada, and K. Fukamichi, *Phys. Rev. B* **66**, 024413 (2002).
- [55] A. J. J. Koch, P. Hokkelling, M. G. v. D. Steeg, and K. J. de Vos, *J. Appl. Phys.* **31**, S75 (1960).
- [56] L. Pareti, F. Bolzoni, F. Leccabue, and A. E. Ermakov, *J. Appl. Phys.* **59**, 3824 (1986).
- [57] P. Wasilewski, *Phys. Earth Planet. Inter.* **52**, 150 (1988).
- [58] S. H. Nie, L. J. Zhu, J. Lu, D. Pan, H. L. Wang, Z. Z. Yu, J. X. Xiao, and J. H. Zhao, *Appl. Phys. Lett.* **102**, 152405 (2013).
- [59] O. N. Mryasov, U. Nowak, K. Y. Guslienko, and R. W. Chantrell, *Europhys. Lett.* **69**, 805 (2005).
- [60] R. F. L. Evans, L. Rózsa, S. Jenkins, and U. Atxitia, *Phys. Rev. B* **102**, 020412(R) (2020).
- [61] R. Cuadrado, R. F. L. Evans, T. Shoji, M. Yano, M. Ito, G. Hrkac, T. Schrefl, and R. W. Chantrell, *J. Appl. Phys.* **130**, 023901 (2021).